# Studying the effects of suberythemal UV doses on human stratum corneum by in vivo confocal Raman spectroscopy

Ali Assi, Sana Tfaili, Alessia Quatela, F. Bonnier, Arlette Baillet-Guffroy, Ali Tfayli

**Full title:** **Studying the effects of suberythemal UV doses on human stratum corneum by *in vivo* confocal Raman spectroscopy**

**Short title:** **Effects of low UV doses on human stratum corneum**

Ali Assi[1], Sana Tfaili[1], Alessia Quatela[2], Franck Bonnier[3], Arlette Baillet-Guffroy[1], Ali Tfayli[1*]

[1] Interdisciplinary Unit: Lipids, Analytical and Biological Systems, Faculty of Pharmacy, Univ. of Paris-Saclay, 5 rue Jean Baptiste Clément, 92296, Châtenay-Malabry. France

[2] Horiba France SAS, 14, Boulevard Thomas Gobert, CS45002, 91120 Palaiseau, France

[3] Université François-Rabelais de Tours, EA 6295 Nanomédicaments et Nanosondes, 31 avenue Monge, 37200 Tours, France

**Keywords:** *In vivo* Raman, stratum corneum, UV radiations, skin lipids, water mobility, proteins secondary structure

*** corresponding author: ali.tfayli@u-psud.fr**

Total number or words: 3335
Total number of figures: 2
Total number of tables: 1
Total number of references: 44

**ABSTRACT**

**Background:** The stratum corneum (SC) plays an important role in the skin barrier function. It acts as a protective barrier against water loss, eliminates foreign substances, micro-organisms and acts against harmful effects of UVR.

**Objectives:** our aim was to study the impacts of $UV_A$ and $UV_B$ exposure in suberythemal doses on molecular structure, organization and barrier function of SC by following different Raman descriptors.

**Materials and methods:** Twenty female volunteers aged from 20 to 30 years with healthy skin were enrolled for the study. 95 mJ/cm² $UV_A$ and 15 mJ/cm² $UV_B$ doses were applied on volunteers' forearms. *In vivo* Raman measurements were performed at irradiated and control regions.

**Results:** The impact of $UV_A$ and $UV_B$ irradiations were observed following several Raman descriptors, *i.e.* the ratio of $v_{asym}CH_2/v_{sym}CH_2$ (2885$cm^{-1}$/ 2850 $cm^{-1}$) for the organizational order of the lipid bilayer. Water content and mobility descriptors were obtained by calculating vOH/vCH ratio. Finally, proteins secondary structure was followed by observing the 1670 $cm^{-1}$/1650 $cm^{-1}$ ratio related to β sheets and α helices respectively.

**Conclusion:** UVA dose induced a loosening of the lateral packing of lipids immediately after irradiation. In contrast, the delayed impact was a tightening of the lipid barrier, an increase in the water content and mainly in the unbound water fraction and higher relative amount of β sheets in SC proteins. Put together, these observations can explain the thickening of the SC observed by previous studies.

15 mJ/cm² $UV_B$ dose was apparently below the threshold to induce significant changes despite the evolution trends that were obtained in this study.

**INTRODUCTION**

The stratum corneum (SC), the outermost layer of the skin represents the main barrier against exogenous insults [1]. It is composed of keratin-filled dead corneocytes embedded in continuous highly organized lipid layers. The unique composition of these lipid layers (ceramides, free fatty acids and cholesterol) plays an important role in the SC function [2]. SC provides thus the first barrier against environmental stresses such as solar radiations and regulates water loss from the body [3].

Solar radiation reaching the surface of the earth, and thereby the surface of our skin, contains infrared (700-2500 nm), visible (400- 700 nm), and ultraviolet radiation (UVR) (290-400 nm) [4]. More precisely, there are three categories of UVR. $UV_C$ rays (200-280 nm) are the shortest in wavelength and are filtered out by the ozone layer. In contrast, $UV_B$ rays (280-320 nm) and $UV_A$ (320-400 nm) reach the earth's surface and are responsible for cutaneous photobiological events. $UV_B$ radiations reach the earth in relatively low amounts (about 0.5% of solar spectral irradiance at ground level, integrated over 290-2500 nm range) and is highly energetic, while $UV_A$ rays are lower in energy, but they are at least 20 times more abundant. 95% of UV rays reaching the ground level are $UV_A$ [4-6].

On one hand, 70% of $UV_B$ radiation that reaches the skin is absorbed by the stratum corneum, 20% reaches viable epidermis, and only 10% penetrates the upper part of the dermis. On the other hand, $UV_A$ radiation is partly absorbed by the epidermis, but 20-30% of it reaches deep dermis. Thus, $UV_A$ rays are more penetrating than $UV_B$ ones. The major chromophores in the skin that determine the depth of penetration are nucleic acids, aromatic amino acids, and melanin. So, $UV_B$ has a major action on the epidermis and $UV_A$ can also reach the dermis [4-7].

Solar UV radiations are known to have beneficial effects on the body such stimulating the production of vitamin D [8]. However, the effect of UV radiations on human health depends on the amount and type of radiation impinging on the body [9].

Penetration of UV light into the skin results in the formation of free radicals, which immediately interact with living cells. Free radicals can cause oxidation effects on epidermal proteins, lipids and epidermal DNA [10-12]. While the roles of $UV_B$ and $UV_A$ wavelengths in the photoaging process and their impacts on the skin are not fully understood, it is known that $UV_A$ radiation contributes significantly to long-term deterioration of the dermal structure and clinical signs of photoaging [13, 14].

Being the first protective barrier of the skin, the SC presents a balanced defense system to protect the body against harmful effects of UVR and the originated free radicals and oxidative reactive species

[10]. This defense mechanism is based of antioxidant substances, such as carotenoids, vitamins, enzymes, and others, which form an antioxidant network of living organism [10].

The impact of $UV_R$ on carotenoids in human skin was performed in vivo using resonance Raman spectroscopy [10, 15]. Darvin et al 2006 [10] and Laderman et al 2011 [15] observed a decrease in beta carotene and lycopene after relatively low $UV_B$ doses exposure with a delay going between 30 to 90 minutes for the former and between 0 and 30 minutes for the latter).

Other components in the SC are highly UV ray absorbing molecules. The Urocanic acid (UCA) can be easily detected in its *trans* form using confocal Raman microscopy [16, 17]. The *trans* form isomerizes to the *cis* form upon UV exposure [16] [17]). In both studies, authors observed a decrease in *trans*-UCA immediately after UV radiation and remained low for one week to regain the initial level about two weeks after [16, 17].

In addition to the effects on UV absorbing molecules, different changes in molecular and biochemical features of the SC were described [18]. For instance, different studies reported an increase in skin thickness [19-21]; *i.e.* Pearse et al. [20] reported since 1987 that both $UV_A$ or $UV_B$ increased the mean epidermal thickness, the mean SC thickness and the mean keratinocytes height significantly. These results, in particular the epidermis thickness were later confirmed by optical coherence tomography (OCT) after repeated $UV_A$ or $UV_B$ doses [21].

The impact of UV exposure on SC lipids was also investigated directly on lipid films [22-25]. Ceramides and fatty acids were exposed to high UV doses. The impact on these lipids can be summarized in three main points, *i.* formation of new entities such as hydroperoxides and epoxides, *ii.* hydrogenation of the double bond, and *iii.* breaking of the carbon chain, leading to rearrangements in alkyl chains of the lipids. [24, 25].

Finally, stratum corneum provides also a critical mechanical protection for the human body [26, 27]. After very high $UV_B$ doses the keratin-controlled stiffness remained constant but the intercellular strength, strain, and cohesion decreased markedly [26, 27]

Here we present the effects of unique $UV_A$ and $UV_B$ exposure in suberythemal doses (95 mJ/cm$^2$ for $UV_A$ and 15 mJ/cm$^2$ for $UV_B$). *In vivo* Raman spectroscopy was used to study the evolution lipids lateral packing and proteins secondary structure. Additionally, we have followed the changes in the water content and water mobility by following the area under curve (AUC) evolution of the OH stretching band.

Impacts of UV radiations were analyzed few minutes after exposure. *In vivo* Raman measurements were repeated at days 2 and 4 in order to follow possible delayed adaptation to UV radiations.

## MATERIALS & METHODS

### Volunteers

Twenty female volunteers aged 20–30 years (mean 25 years) were enrolled in the study. All subjects had no systemic or skin disorders which could influence skin surface pH, hydration and sebum content at the study sites. Volunteers had skin phototypes I and II and were instructed to avoid any skin care product for at least 72 h before the beginning of the experiments. The study was carried out according to ethical principles of the Declaration of Helsinki. All volunteers signed informed consent forms.

### Ultraviolet irradiations

A fiber coupled DH-2000 Deuterium-Halogen light source (215-400 nm) (Ocean Optics, Dunedin, USA) equipped with custom-made $UV_A$ and $UV_B$ bandpass filters were used. Suberythemal $UV_A$ and $UV_B$ doses were applied *i.e.* 95 mJ/cm$^2$ for $UV_A$ (20 minutes exposure) and 15 mJ/cm$^2$ for $UV_B$ (20 seconds exposure).

After an acclimation time of 10 min (22°C, 45% RH), a template containing three apertures ($UV_A$, $UV_B$ and control) of 1 cm$^2$ each in size was attached to the volunteers' volar forearms. Six measurements at different points of the aperture were performed for each volunteer. For intra-individual variability, spectral collection was performed at days 0, 2 and 4 for each volunteer.

### *In vivo* Raman spectroscopy

The *in vivo* Raman microscopic measurements were performed using a confocal Raman optical microprobe (Horiba Jobin Yvon, Villeneuve d'Asc, France) in the range between 400 and 3800 cm$^{-1}$. The utilized excitation wavelength was 660 nm with a laser power on the skin site of 15.0 mW. A long working distance objective MPlan FLN 100X/NA 0.75 was used for focusing the excitation beam and capturing the scattered light. The penetration depth was around 5 µm. Six measurements at different points at the surface of the stratum corneum were performed for each volunteer. For each scan, a 2 s exposure time was used with 2 accumulations.

*In vivo* Raman signatures were collected few minutes after irradiations (D0), 2 days (D2) and 4 days (D4) after UV exposure.

**Data preprocessing and processing**

Signal and spectra have been separated into two wavenumber regions: the so-called fingerprint region i.e. 400-1800 $cm^{-1}$ and the 2600-3100 $cm^{-1}$ region, normalized on Amide I band (1565-1720 $cm^{-1}$) and on C-H stretching band (2800-3030 $cm^{-1}$) respectively.

The different data analysis steps were performed using Matlab (Mathworks, Natick, MA, USA). All spectra were smoothed using Savitzky-Golay algorithm (2th order, 11 points) [28], normalized by applying unit vector method and baseline corrected using an automatic polynomial function [29].

To compare the spectral parameters within each group, the ANOVA test was used. Two-way analysis of variance for variation inter-, intra-groups for all the skin parameters has been presented as mean ± Standard Deviation. Significance limits were set to P-values at 1% and 5%. P-values lower than 10% were used as tendency indicators.

**RESULTS AND DISCUSSION**

**Direct impact of UV radiations**

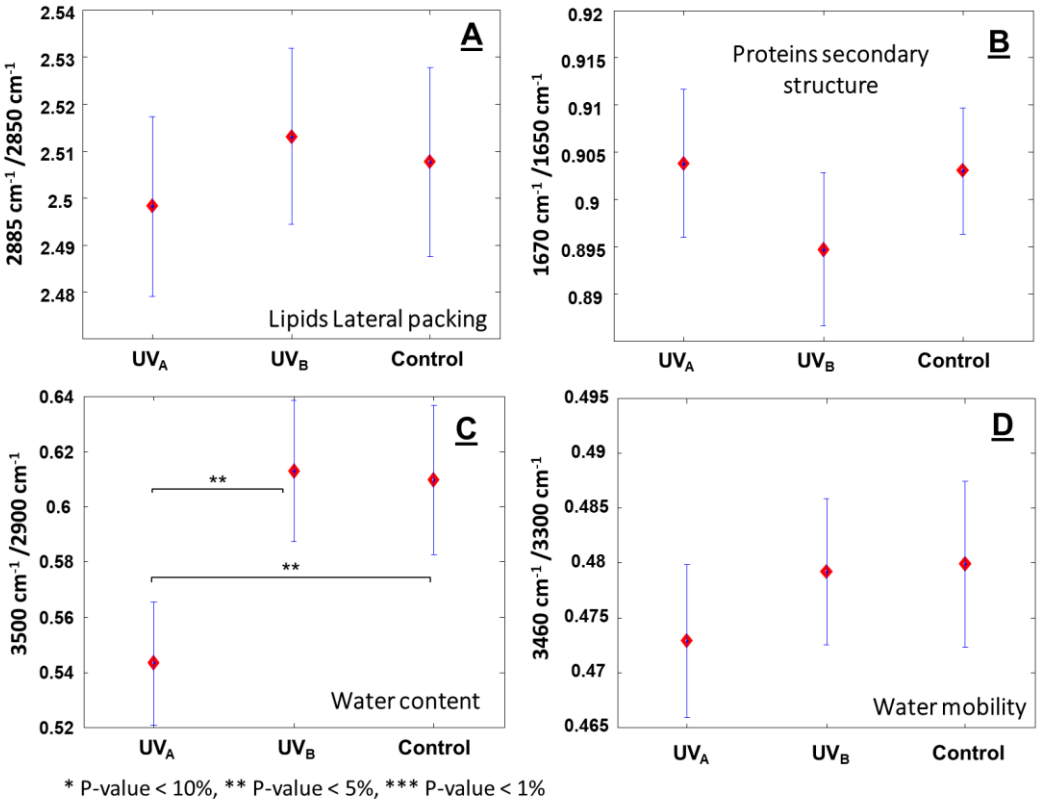


**Fig. 1** Effects of UVA and UVB radiations at D0 few minutes after UV exposure A) $\nu_{asym}CH_2$ (2882 $cm^{-1}$)/$\nu_{sym}CH_2$ (2852 $cm^{-1}$) ratio; B) sub band at 1670 $cm^{-1}$ / band in 1650 $cm^{-1}$ (β sheets / α helices); C) Water content (vOH/vCH Ratio); D) Ratio between unbound water and partially bound water.

As described in the introduction and shown in table 1, *in* vivo Suberythemal doses showed significant effect on SC thickening [20, 21], carotneoids [10, 15] and t-UCA [16, 17]. On hairless mice, TEWL values increased after UV exposure on hairless mice skin [19, 30-32]. FTIR measurements highlighted loosening of the barrier function [32].

In parallel to the SC thickening, Wefers et al. [18] observed, using high performance Thin Layer Chromatography (HPTLC), an increase in the amount of stratum corneum lipids. A result confirmed by Ali S. M. et al. 2014 [33] using Raman spectral imaging after UV exposure.

In contrast to the increase of the SC thickness and lipids amounts, it has been reported that UV exposure induced a loosening in the barrier function [30-32]. All three studies exposed the skin to $UV_B$ rays. As a result , an increased trans-epidermal water loss (TEWL) values were obtained along with abnormalities shown in the bilipid layer with electron microscopy [30], a decrease in covalently bound ceramides [31] and a shift of the $CH_2$ stretching mode in Fourier transform infrared spectroscopy (FTIR) to higher wavenumbers reflecting an increase in the motional freedom of lipids [32]. The two latter modifications peaked between 2 and 4 days after $UV_B$ irradiation.

The direct impact observed on lipid films was obtained with high UV doses UVA (58000 to 1 380 000 000 mJ/cm²) and UVB (150 to 1500 mJ/cm²) (table 1) [22-25]. Modification in the SC lipids were also reported by Biniek et. al. [26] after very high UVB doses (160 000 mJ/cm²).

In addition to the lipidic barrier, tight junctions function as an intercellular permeability barrier mainly against small molecules [34]. It has been shown that $UV_B$ exposure causes functional deterioration of tight junctions [34].

Table 1 presents synthetic summary of the up-mentioned studies against the UVA and UVB used doses. It can be observed that UV doses used for the lipid barrier modification are much higher than minimal erythema doses (MED) for both $UV_A$ (MED ~$4.5.10^3$ mJ/cm²) and $UV_B$ (MED ~150 mJ/cm²) [22-27].

The aim of the present study was to evaluate directly *in vivo*, the effect of suberythemal UV doses on SC barrier function and SC hydration. For $UV_A$, a dose of 95 mJ/cm$^2$ corresponding to 20 minutes of irradiation while for $UV_B$ a 15 mJ/cm$^2$ dose corresponding to 20 seconds of exposure were applied.
To follow lipid compactness the bands at 2850 and 2885 cm$^{-1}$ were measured, and the ratio of the $\nu_{asym}$ $CH_2$ (2885 cm$^{-1}$) to the $\nu_{asym}CH_2$ (2850 cm$^{-1}$) was calculated [35-38]. Despite a very slight decrease tendency on the $UV_A$ exposed zone, no significant changes were observed for both $UV_A$ and $UV_B$ irradiated zones compared to control (figure 01.A).

Hydrogenation of double bonds in lipid chains and breaking carbon chains were reported after UV exposure [22-25]. The ν=CH/$\nu CH_2$ ratio (3060 $cm^{-1}$/(2850 +2885 $cm^{-1}$)) and the $\nu CH_3/\nu CH_3$ ratio were calculated to monitor double bonds hydrogenation and modifications in the alkyl chains lengths respectively (data not shown). No significant modifications were obtained.

The Amide I band is directly related to the secondary structure of proteins. It can be composed into several sub-bands associated with different forms of secondary structure; i.e. α helix, ß sheet, turns and random coil structures. The sub-band around 1650 $cm^{-1}$ is associated with α helix form of the keratin, while the sub-band arising around 1670 $cm^{-1}$ was assigned to β sheets. Finally, the 1690 $cm^{-1}$ feature was attributed to turns and random coils [39-43]. No modifications were detected immediately after UV exposure (figure 01.B). Similar results were obtained for proteins folding (data not shown) by following the maximum position of $\nu CH_3$ band around (2930 $cm^{-1}$).

Global water content in the SC was evaluated using the AUC of the OH stretching (νOH) band (3100-3700 $cm^{-1}$). The spectral region 3250-3450$cm^{-1}$ is associated to partially bound water while the vibrations in the 3450-3600$cm^{-1}$ region are due to unbound water [38, 39, 41-44]. Water content decreased significantly (P-value < 0.05) after $UV_A$ irradiation (figure 01.C). This decrease is accompanied with a non-significant decrease in unbound to partially bound water ratio (figure 01.D). No significant variations on water content or mobility were observed after $UV_B$ exposition. A possible explanation may be related to the exposure time to obtain the wanted dose (20 seconds for $UV_B$ against 20 minutes for $UV_A$).

| | Reference | UV dose (mJ/cm²) | | Number of UV exposure | Technique / methodology | Observations |
|---|---|---|---|---|---|---|
| | | $UV_A$ | $UV_B$ | | | |
| *In vivo*, human | Darvin et al 2006 [10] | | 30 mJ/cm² | 1 | Resonant Raman spectroscopy | decrease in beta carotene and lycopene |
| *In vivo*, human | Laderman et al 2011 [15] | | 30 mJ/cm² | 1 | Resonant Raman spectroscopy | |
| *In vivo*, human | Egawa et al. 2008 [17] | | 25 mJ/cm² | 1 | confocal Raman microscopy | decrease in *trans*-UCA |
| *In vivo*, human | Tosato et al. 2015[16] | | 1300 mJ/cm² | 1 | confocal Raman microscopy | |
| *In vivo*, human | Pearse et al. 1987 [20] | $6.10^3$ mJ/cm² per dose | 75, 150 and 300 mJ/cm² | $UV_B$ 3 times weekly for 6 weeks (total of 16 times) $UV_A$: 9 times | Biopsies, Histochemical reactions Image analyses | increase in mean epidermis thickness, SC thicknesses and mean keratinocytes height |
| *In vivo*, human | Gambichler et al. 2005 [21] | $6.10^4$ mJ/cm² per dose | 200 mJ/cm² per dose | 3 days | Optical coherence tomography | increase in Epidermis thickness |
| *In vivo*, human | Wefers et al. 1991 [18] | $5.10^4$ J/cm² | 124±39 mJ/cm² | 3 times weekly for 3 weeks | Thin-layer Chromatography (HPTLC) | increase in the amount of Stratum Corneum lipids |
| Human skin biopsies and reconstructed human skin | Ali S. M. 2014 [33] | 9500 to $7.6.10^4$ mJ/cm² | 390 to 3140 mJ/cm² UVB | 1 | Raman spectroscopy, histological profiling | |
| *In vivo*, hairless mice | Meguro et al. 1999 [30] | | 40 mJ/cm² | Once per day for 15 days | TEWL Electron microscopy on sections | Increased TEWL abnormalities in the bilipid layer |
| *Ex vivo*, hairless mice | Gélis et al. 2002 [19] | | 21, 105, 210 and 420 mJ/cm² | 1 | TEWL Follow-up of the penetration of tritiated water and $^{14}C$ caffeine | Increased TEWL Higher permeability |
| *In vivo*, hairless mice | Takagi Y. et al. 2004 [31] | | 18, 37 and 75 mJ/cm² | 1 | TEWL Lipids extraction HPTLC RT-PCR | Increased TEWL decrease in covalently bound ceramides |
| *In vivo*, hairless mice | Jun Jiang et al. 2006 [32] | | 150 mJ/cm² | 1 | FTIR TEWL Electron microscopy | Increased TEWL Higher motional freedom of lipids |

| | | | | | | |
|---|---|---|---|---|---|---|
| *Human skin xenographs. And keratinocytes cultures* | Yuki et al. 2010 [34] | | 40 and 200 mJ/cm² for xenographs 10 to 40 mJ/cm² for keratinocytes culture | | Immunofluorescence microscopy Rac activation assay Tj permeability assay with biotinylation technique | functional deterioration of tight junctions |
| Lipids | Trommer et al. 2001 [22] | $5.8.10^4$ to $13.8.10^8$ mJ/cm² | | | mass spectrometry | formation of new oxidative entities hydrogenation of double bonds Breaking of carbon chains |
| Lipids | Trommer et al. 2002 [23] | | 250 mJ/cm² | | HPLC-MS: Electron Paramagnetic Resonance | |
| Ceramides and fatty acids films | 2008, Merle et al. [24] | $6.10^4$ and $12.10^4$ mJ/cm² | | | FTIR Mass spectrometry | |
| Ceramides and fatty acids films | 2010, Merle et al. [25], | $120.10^3$ mJ/cm² | 150 and 1500 mJ/cm² | | FTIR Mass spectrometry | |
| Stratum corneum | Biniek et al. [26] | | $16.10^4$ mJ/cm² | | | keratin-controlled stiffness remained constant intercellular strength, strain, and cohesion decreased |
| Stratum corneum | 2019, Berkey et al. [8] | | $5.10^3$, $30.10^3$, $125.10^3$ and $265.10^3$ mJ/cm² | | | |

Table 01: Summary of different studies (*in vivo* and *ex vivo*) of impacts of UVR on the skin structure and composition using different methods and dose

**Delayed impact of UV radiations**

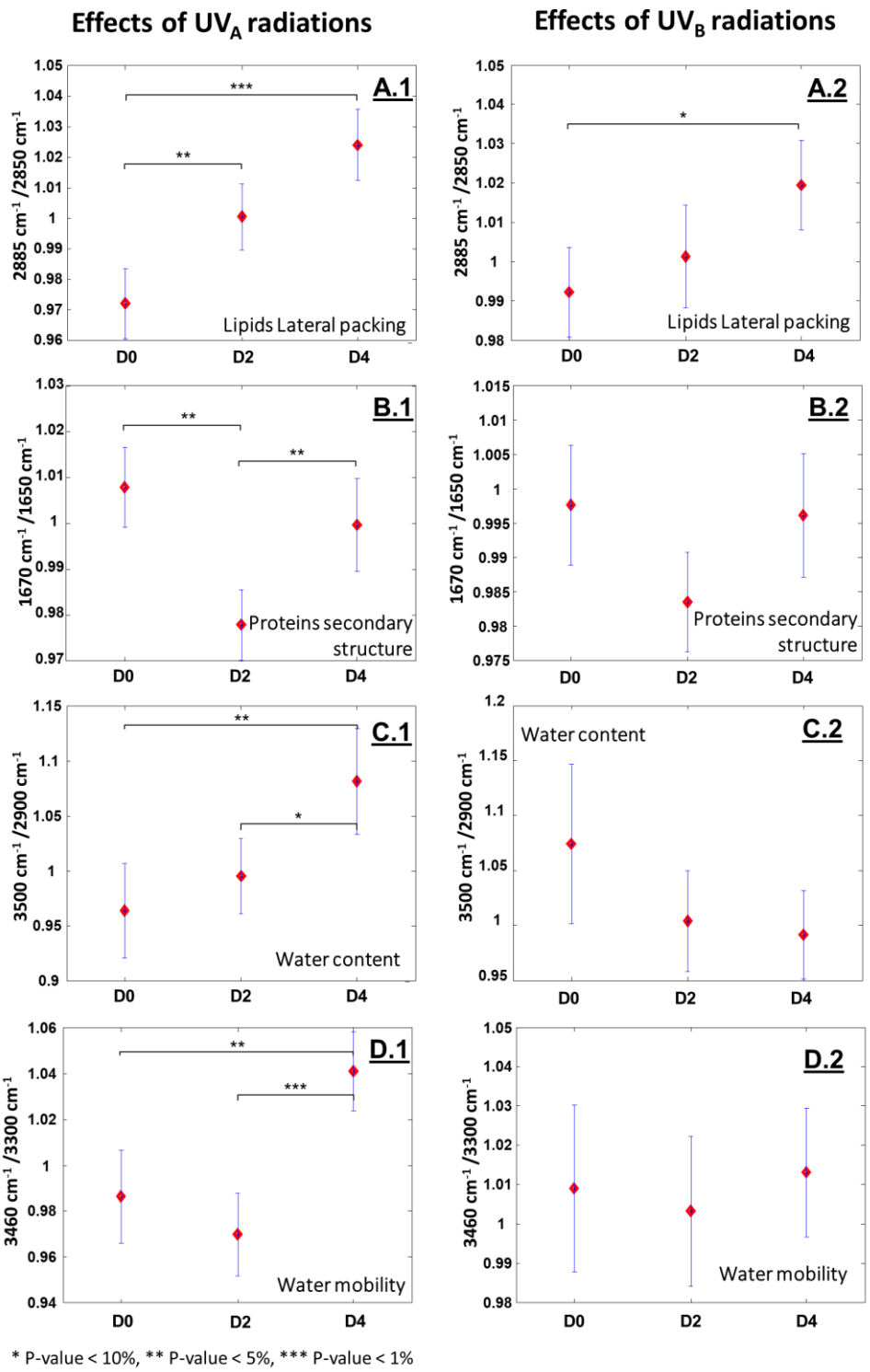


**Fig. 2** Delayed effects of UV$_A$ (.1) and UV$_B$ (.2) radiations. A) $\nu_{asym}CH_2$ (2882 cm$^{-1}$)/$\nu_{sym}CH_2$ (2852 cm$^{-1}$) ratio; B) sub band at 1670 cm$^{-1}$ / band in 1650 cm$^{-1}$ (β sheets / α helices); C) Water content (vOH/vCH Ratio); D) Ratio between unbound water and partially bound water

Raman measurements collected few minutes after UV irradiations revealed the direct impact of UV energy absorbed by molecular patterns within the SC. Thus, when using very low UV doses it was expected to have no marked trends between UV exposed and control zones of the skin.

Meanwhile, several studies reported delayed of UV exposure. For instance, maximum modifications were observed 30-90 minutes after irradiation for β-carotene [10, 15], 2- 4 days for TEWL (observed on hairless mice skin) [32] and 1 week for t-UCA [16, 17].

We have therefore collected *in vivo* Raman signatures at the surface of irradiated and control zones 2 and 4 days after exposure. In order to avoid the large inter-individual variability and inter-days physiological variations for each volunteer, each spectral descriptor obtained from the $UV_A$ and $UV_B$ irradiated areas was expressed as a function of the control area (figure 2). Thus, for a given descriptor, a value close to one is indicative to zero changes between irradiated and control.

Double bonds monitoring and $CH_3/CH_2$ ratio showed no changes on both $UV_A$ and $UV_B$ irradiated zones compared to control (data not shown).

Figure 2.1 shows the effects of 95 mJ/cm² dose of $UV_A$ radiations at D0, D2 and D4. A complex evolution of the different molecular descriptors can be observed. A slight decrease tendency was observed in the lipids lateral packing at D0 for $UV_A$ (figures 1.A and 2.A.1). Significant increase in the $\nu_{asym}CH_2/\nu_{sym}CH_2$ ratio at D2 (D0-D2 P-value < 0.05) and D4 (D0-D4 P-value < 0.01) was observed revealing higher organization of the lipidic bilayer in the SC (figure 2.A.1).

As a direct consequence of the higher lipidic barrier function, global water content showed an increase trend at D2 followed by a significant increase at D4 (D0-D4 P-value < 0.05) (figure 2.C.1). This was due to better barrier against water loss.

The observation of the water mobility (figure 2.D.1) showed significant increase at D4 (D0-D4 P-value < 0.05). This can be directly related to a higher lipidic barrier against water loss which will mainly affect unbound water content.

Meanwhile, 2 days after $UV_A$ exposure the relative amount of unbound water showed a non-significant decrease compared to partially bound water (figure 2.D.1). This can be explained by a complex equilibrium between three molecular patterns within SC *i.e.* lipids lateral packing, proteins secondary structure and water mobility. At D2, a relative decrease in β sheets was observed (figure 2.B.1). Previous studies on skin drying process showed simultaneous evolution of β sheets and unbound / partially bound water ratios [38, 39, 41-44].

At Day 4, increased water holding capacity and consequently the water content induced an increase in the volume of the SC. This latter can explain the re-equilibrium between β sheets/ α helices ratio. This could be the origin of the reported thickening of SC after $UV_A$ exposure (table 1) [19-21]. TEWL and

corneometry measurments (Data not shown) seemed to be less sensitive than Raman and showed no significant variations.

At low doses, $UV_B$ radiation did not show significant effects on the SC molecular structures (figure 2.2). However, the most significant trend was observed in the lipids' compactness (Fig. 2.A.2) (p-value 0.08). It is worthy to notice the similar evolution (even non-significant) trends for lipids lateral packing and proteins secondary structure for both $UV_A$ and $UV_B$. In contrast, a very slight non-significant decrease tendency of water content was observed (figure 2.C.2).

The used $UV_B$ dose obtained after only 20 seconds of irradiation may be below the threshold dose necessary to induce significant changes in SC features.

The significant modifications obtained at D2 and D4 may be due to indirect impact of $UV_A$ which can go deeper than $UV_B$ and thus could trigger a defensive process that leads to an enhancement in the lipid's barrier.

**Conclusion**

The aim of this study was to explore the impact of low UV doses on SC molecular patterns. A 95 mJ/cm² $UV_A$ dose induced a loosening of the lateral packing of lipids immediately after irradiation. In contrast, the delayed impact was a tightening of the lipid barrier that conducted to an increase in the water content and mainly in the unbound water fraction. Higher water content resulted into bigger SC volume (hydrated SC) which is generally accompanied with higher relative amount of β sheets in SC proteins. Put together, these observations can explain the thickening of the SC observed by previous studies [19-21]. Based on these observations, one could suggest that UVA at low doses may have a positive impact on the SC barrier function.

15 mJ/cm² UVB dose was apparently below the threshold to induce significant changes despite the evolution trends that were obtained in this study. Further investigations should be performed with gradually higher $UV_B$ doses.

**References**


1. Nicolaou A, Pilkington SM, Rhodes LE. Ultraviolet-radiation induced skin inflammation: dissecting the role of bioactive lipids. *Chem Phys Lipids*. 2011; 164(6): 535-43. doi: 10.1016/j.chemphyslip.2011.04.005
2. Gruber F, Kremslehner C, Narzt M-S. The impact of recent advances in lipidomics and redox lipidomics on dermatological research. *Free Radical Biology and Medicine*. 2019; 144: 256-65. doi: 10.1016/j.freeradbiomed.2019.04.019
3. Natarajan VT, Ganju P, Ramkumar A, Grover R, Gokhale RS. Multifaceted pathways protect human skin from UV radiation. *Nature Chemical Biology*. 2014; 10(7): 542-51. doi: 10.1038/nchembio.1548
4. Johnson BE. The influence of radiation on the skin and the basis of protection. *International Journal of Cosmetic Science*. 1983; 5(4): 131-9. doi: 10.1111/j.1467-2494.1983.tb00334.x

5. Amaro-Ortiz A, Yan B, D'Orazio J. Ultraviolet Radiation, Aging and the Skin: Prevention of Damage by Topical cAMP Manipulation. *Molecules*. 2014; 19(5): 6202-19. doi: 10.3390/molecules19056202
6. Couteau C, Couteau O, Alami-El Boury S, Coiffard LJM. Sunscreen products: What do they protect us from? *International Journal of Pharmaceutics*. 2011; 415(1-2): 181-4. doi: 10.1016/j.ijpharm.2011.05.071
7. Battie C, Verschoore M. Cutaneous solar ultraviolet exposure and clinical aspects of photodamage. *Indian Journal of Dermatology, Venereology, and Leprology*. 2012; 78(7): 9. doi: 10.4103/0378-6323.97350
8. Berkey C, Oguchi N, Miyazawa K, Dauskardt R. Role of sunscreen formulation and photostability to protect the biomechanical barrier function of skin. *Biochemistry and biophysics reports*. 2019; 19: 100657. doi: 10.1016/j.bbrep.2019.100657
9. Lucas R, McMichael T, Smith W, Armstrong B. *Solar Ultraviolet Radiation: Global burden of disease from solar ultraviolet radiation*. Annette P-Ü, Hajo Z, Colin M, Michael R, editors. Geneva World Health Organization 2006.
10. Darvin ME, Gersonde I, Albrecht H, Sterry W, Lademann J. In vivo Raman spectroscopic analysis of the influence of UV radiation on carotenoid antioxidant substance degradation of the human skin. *Laser Physics*. 2006; 16(5): 833-7. doi: 10.1134/S1054660X06050148
11. Gonzaga ER. Role of UV Light in Photodamage, Skin Aging, and Skin Cancer. *American Journal of Clinical Dermatology*. 2009; 10(Supplement 1): 19-24. doi: 10.2165/0128071-200910001-00004
12. Nicolaou A, Pilkington SM, Rhodes LE. Ultraviolet-radiation induced skin inflammation: dissecting the role of bioactive lipids. *Chemistry and Physics of Lipids*. 2011; 164(6): 535-43. doi: 10.1016/j.chemphyslip.2011.04.005
13. Villaret A, Ipinazar C, Satar T, *et al.* Raman characterization of human skin aging. *Skin Research and Technology*. 2018; 25(3): 270-6. doi: 10.1111/srt.12643
14. Scharffetter–Kochanek K, Brenneisen P, Wenk J, *et al.* Photoaging of the skin from phenotype to mechanisms. *Experimental Gerontology*. 2000; 35(3): 307-16. doi: 10.1016/s0531-5565(00)00098-x
15. Lademann J, Schanzer S, Meinke M, Sterry W, Darvin ME. Interaction between carotenoids and free radicals in human skin. *Skin Pharmacol Physiol*. 2011; 24(5): 238-44. doi: 10.1159/000326074
16. Tosato MG, Orallo DE, Ali SM, Churio MS, Martin AA, Dicelio L. Confocal Raman spectroscopy: In vivo biochemical changes in the human skin by topical formulations under UV radiation. *Journal of photochemistry and photobiology B, Biology*. 2015; 153: 51-8. doi: 10.1016/j.jphotobiol.2015.08.030
17. Egawa M, Iwaki H. In vivo evaluation of the protective capacity of sunscreen by monitoring urocanic acid isomer in the stratum corneum using Raman spectroscopy. *Skin Res Technol*. 2008; 14(4): 410-7.
18. Wefers H, Melnik BC, Flur M, Bluhm C, Lehmann P, Plewig G. Influence of UV irradiation on the composition of human stratum corneum lipids. *J Invest Dermatol*. 1991; 96(6): 959-62.
19. Gelis C, Mavon A, Delverdier M, Paillous N, Vicendo P. Modifications of in vitro skin penetration under solar irradiation: evaluation on flow-through diffusion cells. *Photochem Photobiol*. 2002; 75(6): 598-604. doi: 10.1562/0031-8655(2002)075<0598:moivsp>2.0.co;2
20. Pearse AD, Gaskell SA, Marks R. Epidermal Changes in Human Skin Following Irradiation With Either UVB or UVA. *Journal of Investigative Dermatology*. 1987; 88(1): 83-7. doi: 10.1111/1523-1747.ep12465094
21. Gambichler T, Kunzlberger B, Paech V, *et al.* UVA1 and UVB irradiated skin investigated by optical coherence tomography in vivo: a preliminary study. *Clinical and Experimental Dermatology*. 2005; 30(1): 79-82. doi: 10.1111/j.1365-2230.2004.01690.x
22. Trommer H. The examination of skin lipid model systems stressed by ultraviolet irradiation in the presence of transition metal ions. *European Journal of Pharmaceutics and Biopharmaceutics*. 2001; 51(3): 207-14. doi: 10.1016/s0939-6411(01)00140-0
23. Trommer H, Bottcher R, Poppl A, Hoentsch J, Wartewig S, Neubert RH. Role of ascorbic acid in stratum corneum lipid models exposed to UV irradiation. *Pharm Res*. 2002; 19(7): 982-90.
24. Merle C, Laugel C, Baillet-Guffroy A. Spectral monitoring of photoirradiated skin lipids: MS and IR approaches. *Chem Phys Lipids*. 2008; 154(1): 56-63.
25. Merle C, Laugel C, Baillet-Guffroy A. Effect of UVA or UVB irradiation on cutaneous lipids in films or in solution. *Photochem Photobiol*. 2010; 86(3): 553-62.
26. Biniek K, Levi K, Dauskardt RH. Solar UV radiation reduces the barrier function of human skin. *Proc Natl Acad Sci U S A*. 2012; 109(42): 17111-6.
27. Zanyar M, Rehman S, Rehamn I. Raman spectroscopy of biological tissues. *Appl Spectrosc*. 2007; 42(5): 493-541. doi: 10.1080/05704920701551530
28. Savitzky A, Golay MJE. Smoothing and differentiation of data by simplified least squares procedures. *Anal Chem*. 1964; 36: 1627-39.
29. Zhao J, Lui H, McLean DI, Zeng H. Automated autofluorescence background subtraction algorithm for biomedical Raman spectroscopy. *Appl Spectrosc*. 2007; 61(11): 1225-32.
30. Meguro S, Arai Y, Masukawa K, Uie K, Tokimitsu I. Stratum corneum lipid abnormalities in UVB-irradiated skin. *Photochem Photobiol*. 1999; 69(3): 317-21. doi: 10.1562/0031-8655(1999)069<0317:caiuis>2.3.co;2

31. Takagi Y, Nakagawa H, Kondo H, Takema Y, Imokawa G. Decreased levels of covalently bound ceramide are associated with ultraviolet B-induced perturbation of the skin barrier. *J Invest Dermatol*. 2004; 123(6): 1102-9. doi: 10.1111/j.0022-202X.2004.23491.x
32. Jiang SJ, Chen JY, Lu ZF, Yao J, Che DF, Zhou XJ. Biophysical and morphological changes in the stratum corneum lipids induced by UVB irradiation. *Journal of Dermatological Science*. 2006; 44(1): 29-36. doi: 10.1016/j.jdermsci.2006.05.012
33. Ali SM, Bonnier F, Ptasinski K, *et al.* Raman spectroscopic mapping for the analysis of solar radiation induced skin damage. *Analyst*. 2013; 138(14): 3946-56.
34. Yuki T, Hachiya A, Kusaka A, *et al.* Characterization of Tight Junctions and Their Disruption by UVB in Human Epidermis and Cultured Keratinocytes. *Journal of Investigative Dermatology*. 2011; 131(3): 744-52. doi: 10.1038/jid.2010.385
35. Tfayli A, Guillard E, Manfait M, Baillet-Guffroy A. Thermal dependence of Raman descriptors of ceramides. Part I: effect of double bonds in hydrocarbon chains. *Anal Bioanal Chem*. 2010; 397(3): 1281-96. doi: 10.1007/s00216-010-3614-y
36. Guillard E, Tfayli A, Manfait M, Baillet-Guffroy A. Thermal dependence of Raman descriptors of ceramides. Part II: effect of chains lengths and head group structures. *Anal Bioanal Chem*. 2011; 399(3): 1201-13. doi: 10.1007/s00216-010-4389-x
37. Tfayli A, Guillard E, Manfait M, Baillet-Guffroy A. Molecular interactions of penetration enhancers within ceramides organization: a Raman spectroscopy approach. *Analyst*. 2012; 137(21): 5002-10. doi: 10.1039/c2an35220f
38. Tfayli A, Jamal D, Vyumvuhore R, Manfait M, Baillet-Guffroy A. Hydration effects on the barrier function of stratum corneum lipids: Raman analysis of ceramides 2, III and 5. *Analyst*. 2013; 138(21): 6582-8. doi: 10.1039/c3an00604b
39. Vyumvuhore R, Tfayli A, Duplan H, Delalleau A, Manfait M, Baillet-Guffroy A. Effects of atmospheric relative humidity on stratum corneum lipids and proteins structures. Raman spectroscopy analysis. *International Journal of Cosmetic Science*. 2012; 34(4): 386-.
40. Vyumvuhore R, Tfayli A, Duplan H, Delalleau A, Manfait M, Baillet-Guffroy A. Raman spectroscopy: a tool for biomechanical characterization of Stratum Corneum. *Journal of Raman Spectroscopy*. 2013; 44(8): 1077-83.
41. Vyumvuhore R, Tfayli A, Duplan H, Delalleau A, Manfait M, Baillet-Guffroy A. Effects of atmospheric relative humidity on Stratum Corneum structure at the molecular level: ex vivo Raman spectroscopy analysis. *Analyst*. 2013; 138(14): 4103-11. doi: 10.1039/c3an00716b
42. Vyumvuhore R, Tfayli A, Biniek K, *et al.* The relationship between water loss, mechanical stress, and molecular structure of human stratum corneum ex vivo. *J Biophotonics*. 2015; 8(3): 217-25. doi: 10.1002/jbio.201300169
43. Biniek K, Tfayli A, Vyumvuhore R, *et al.* Measurement of the Biomechanical Function and Structure of Ex Vivo Drying Skin Using Raman Spectral Analysis and its Modulation with Emollient Mixtures. *Exp Dermatol*. 2018; 27(8): 901-8. doi: 10.111/exd.13721
44. Vyumvuhore R, Tfayli A, Manfait M, Baillet-Guffroy A. Vibrational spectroscopy coupled to classical least square analysis, a new approach for determination of skin moisturizing agents' mechanisms. *Skin Res Technol*. 2014; 20(3): 282-92. doi: 10.1111/srt.12117